International Journal of Heat and Technology
Vol. 42, No. 2, April, 2024, pp. 511-519
Journal homepage: http://iieta.org/journals/ijht

Mixed Convection in an Open Cavity with an Internal Fin Filled with Nanofluid in a Porous Medium Using Two-Phase Mixture Model

Tabti Wissame*, Bessaïh Rachid

LEAP Laboratory, Mechanical Engineering Department, University of Mentouri Brothers-Constantine 1, Constantine 25000, Algeria

Corresponding Author Email: bessaih.rachid@umc.edu.dz

https://doi.org/10.18280/ijht.420217

Received: 30 October 2023
Revised: 10 March 2024
Accepted: 18 March 2024
Available online: 30 April 2024

Keywords:
mixed convection, nanofluid, porous media, two-phase model

ABSTRACT

This study investigates the mixed convection of Cu-water nanofluid in an open square cavity with an internal fin and a porous medium, using the two-phase mixture model. Though all the walls in the cavity are assumed to be insulated, the bottom wall, where the fin is attached, is evenly heated. The simulation examines the impact of varying Darcy numbers ($Da=10^{-1}$, 10^{-2}, 10^{-3}, and 10^{-4}), porosity ($\varepsilon=0.2$, 0.4, 0.6, and 0.8), and solid volume fraction ($0\leq\varphi\leq0.08$) on Nusselt, entropy generation, and Bejan numbers. S_{gen} decreases as the Da increases, but Nu_{avg} and Be increase—quite the opposite of expectations. Reducing material porosity increases heat transfer. Finally, incorporating nanofluid into heat transfer systems could lead to significant improvements in heat transfer efficiency. These findings provide practical guidance for optimizing material properties to achieve desired heat transfer characteristics.

1. INTRODUCTION

Enhancing heat transfer refers to improving the rate and efficiency of thermal transfer between two or more objects or mediums. Efficient heat transfer is crucial in various industrial, technological, and everyday applications to optimize performance, increase energy efficiency, and prevent overheating. Heat transfer can be improved when pure fluids are used instead of nanofluids. Base fluids like water, oil, or ethylene glycol are mixed with high thermally conductive metallic or non-metallic nanoparticles like Cu, Al, Al_2O_3, SiO_2, etc. [1, 2]. The problem of mixed convection in different cavity shapes with varying boundary conditions filled with nanofluid has gained significant interest over the years [3-6]. Through all these studies, they discovered that mixed convection across cavities is significantly impacted by flow direction, cavity steering, obstacle existence, and fluid characteristics on heat transfer rate. Hence, Selimefendigil and Öztop [7] studied the mixed convection in an enclosure containing two inner adiabatic spinning circular cylinders utilizing various types of nanoparticles. They concluded that the nanofluid provides a better heat transfer rate than other particles, equal to 4 percent when the Rayleigh number is high. In a square cavity that had a complicated fin, Shulepova et al. [8] Simulated the mixed convection of an Al_2O_3-water nanofluid. They mentioned that the heat transfer intensity was influenced by both the interior block's position and the nanoparticles' concentration. Ching-Chang-Cho [9] studied nanofluid mixed convection and entropy generation in a lid-driven cavity. According to his findings, there is a correlation between the amount of nanoparticle and an increase in the Nu_{avg} as well as total entropy production. Hussain et al. [10] performed a computational investigation into the mixed convection of a hybrid nanofluid within an open cavity that included an adiabatic obstacle. More studies that are comparable to this one has been carried out using a variety of nanofluids [11-13].

Because of the presence of interconnected pores that provide a large surface area for fluid-solid interaction, using porous mediums is another method for enhancing heat transfer in nanofluid thermal systems. This method helps improve the convective heat transfer. Porous mediums can be found in materials like porous media. Olak et al. [14] investigated a problem involving mixed convection conditions in a cavity driven by a lid and containing a heated porous block. They discovered that a reduction in Darcy's number could lead to an increase in the Nu_{avg}. In their study, Sheremet et al. [15] investigated the impact of Darcy's number and the dimensions of the inlet and outlet sections in the context of utilizing mixed convection within an open square cavity containing nanofluid. They have discovered an improvement in heat transfer after making the parameter adjustments. Laminar mixed convection was investigated by Tham et al. [16] over a circular cylinder. Siavashi et al. [17], conducted a study on the natural convection flow of a nanofluid composed of copper and water. Their investigation was carried out within a cavity featuring a set of fins attached to the heated wall. The researchers used the two-phase method for their investigation. They discovered that incorporating porous fins with high Darcy numbers improved heat transfer and that the opposite was true. Rajarathinam et al. [18] predicted Cu-water nanofluid mixed convection in an inclined porous cavity. They considered the effects of the moving wall(s) direction with three different cases and discovered that it plays a major role in flow and heat transfer. Using the two-phase mixture model, Emami et al. [19]

investigated the natural convection of Cu-water nanofluid within an inclined porous cavity. They did this by observing the flow of the nanofluid. According to the results of their investigation, the positioning of the hot wall has a significant bearing on how the inclination angle is behaved. If you have a square and tilted cavity at an angle, it might be advantageous in some circumstances; however, in other circumstances, the overall heat transfer would be reduced.

According to the comprehensive review of the relevant literature that was discussed earlier, it is abundantly clear that the scenario of mixed convection utilizing the two-phase model in an open cavity that is both filled with Cu-water nanofluid and contains an internal fin that is covered with a porous medium has not been given any consideration or investigated. We discussed this topic and investigated how important factors, such as the Da number, affect the amount of heat transferred via convection.

2. GEOMETRY DESCRIPTION

The considered geometry for our study is a 3D cubical cavity of size L with an internal fin heated from the bottom wall (T_h) and covered with a porous layer, as shown in Figure 1. The remaining walls are thermally insulated, and the flow enters the cavity with an initial velocity of U_o and temperature of T_o.

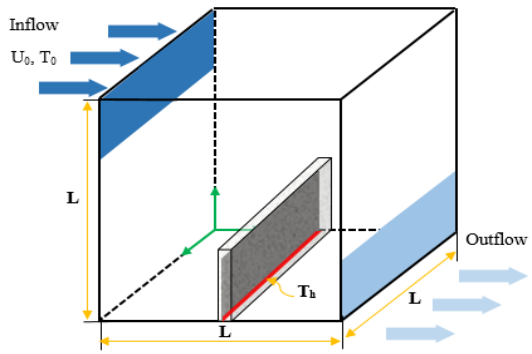

Figure 1. Cavity geometry

The nanofluid is thought to be Newtonian, laminar, and the Boussinesq method is applied. The characteristics of the water and the material are illustrated in Table 1.

Table 1. Thermal properties of water and copper

Properties	Pure Water	Copper (Cu)
ρ (Kg/m^3)	997.1	8933
Cp (J/Kg.K)	4179	385
β (K^{-1})	21×10^{-5}	1.67×10^{-5}
k (W/m.K)	0.613	401
μ (Kg/m.s)	0.001003	/

3. MATHEMATICAL FORMULATION

The fluid is Newtonian, permanent, and incompressible; the flow of fluid within the cavity is laminar and three-dimensional; and the local thermal equilibrium between the fluid and the porous medium is verified.

The steady-state mixture model is governed by continuity, momentum, energy, and entropy production equations [20]:

$$\nabla.(\rho_m \mathrm{V}_m) = 0 \tag{1}$$

$$\nabla.(\rho_m V_m V_m) = -\nabla \mathrm{P} + \nabla.(\nabla \mathrm{V}_m + \nabla_m^T)\mu_m + \nabla \sum_{k=1}^{n}(\rho_k \varphi_k V_{dr,k} V_{dr,k}) - F_{np} + (\rho\beta)_m(T - T_i)\mathrm{g} \tag{2}$$

$$\nabla.\sum_{k=1}^{n}(\rho_k\, \varphi_k V_k C_{p,k} T) = \nabla.(\mathrm{K}_m \nabla T) \tag{3}$$

$$\nabla.(\varphi_{nf}\rho_{nf}\mathrm{V}_m) = \nabla.(\varphi_{nf}\rho_{nf}\mathrm{V}_{dr,np}) \tag{4}$$

where, $\mathrm{V}_m, \mathrm{V}_{dr,k}, \mathrm{V}_{np,f}$ are respectively the mixture, drift, and slip velocities and represented as follows [21]:

$$\mathrm{V}_m = \sum_{k=1}^{n} \frac{\varphi_k \rho_k \mathrm{V}_k}{\rho_m} \tag{5}$$

$$\mathrm{V}_{dr,k} = \mathrm{V}_k - \mathrm{V}_m \tag{6}$$

$$\mathrm{V}_{np,f} = \mathrm{V}_{np} - \mathrm{V}_f \tag{7}$$

Relationship between drift and relative velocity:

$$\mathrm{V}_{dr,np} = \mathrm{V}_{np,f} - \sum_{k=1}^{n} \frac{\varphi_k \rho_k \mathrm{V}_k}{\rho_m} \tag{8}$$

$$\mathrm{V}_{np,f} = \frac{\rho_p d_p^2}{\mu_f f_{drag}} \frac{(\rho_{np} - \rho_m)}{\rho_{np}} g - (\mathrm{V}_m.\nabla)\mathrm{V}_m \tag{9}$$

$$f_{drag} = \begin{cases} 1 + 0.15\mathrm{Re}_p^{0.687}, \mathrm{Re}_p \le 1000 \\ 0.0183\mathrm{Re}_p \quad\quad , \mathrm{Re}_p \ge 1000 \end{cases} \tag{10}$$

$$\mathrm{F}_{np} = \Sigma_{k=1}^{2} \varphi_k \left(\frac{\mu_k}{\mathrm{K}_k} u_k + \frac{C_{d,k}\rho_k}{\sqrt{\mathrm{K}_k}} |u_k|\right) \tag{11}$$

where, C_d and k are the inertia coefficient and permeability of the porous medium and calculated as:

$$C_d = \frac{1.75}{\sqrt{150}\varepsilon^{3/2}} \tag{12}$$

$$k = \frac{\varepsilon^3 D_{np}^2}{150(1-\varepsilon)^2} \tag{13}$$

The entropy is generated as a result of irreversibility source in the flow field, such as the viscous dissipation effect and heat transfer, as per the method suggested by Bejan [22], S_{gen} can be calculated using the formula [23]:

$$S_{gen} = S_{gen,T} + S_{gen,f} \tag{14}$$

where, $S_{gen,T}$ represents the entropy generation rate caused by the heat transfer irreversibility and is defined as:

$$S_{gen,T} = \frac{k_m}{T^2}\left[\left(\frac{\partial T}{\partial x}\right)^2 + \left(\frac{\partial T}{\partial y}\right)^2 + \left(\frac{\partial T}{\partial z}\right)^2\right] \tag{15}$$

$S_{gen,f}$ is the entropy production attributed to fluid friction given by:

For the clear region:

$$S_{gen,f} = \frac{\mu_m}{T_o}\left\{2\left[\left(\frac{\partial u}{\partial x}\right)^2 + \left(\frac{\partial v}{\partial y}\right)^2 + \left(\frac{\partial w}{\partial z}\right)^2\right] + \left(\frac{\partial u}{\partial y} + \frac{\partial v}{\partial x}\right)^2 + \left(\frac{\partial v}{\partial z} + \frac{\partial w}{\partial y}\right)^2 + \left(\frac{\partial w}{\partial x} + \frac{\partial u}{\partial z}\right)^2\right\} \quad (16)$$

For the porous region:

$$S_{gen,f} = \frac{\mu_m}{T_o}\left\{2\left[\left(\frac{\partial u}{\partial x}\right)^2 + \left(\frac{\partial v}{\partial y}\right)^2 + \left(\frac{\partial w}{\partial z}\right)^2\right] + \left(\frac{\partial u}{\partial y} + \frac{\partial v}{\partial x}\right)^2 + \left(\frac{\partial v}{\partial z} + \frac{\partial w}{\partial y}\right)^2 + \left(\frac{\partial w}{\partial x} + \frac{\partial u}{\partial z}\right)^2\right\} + \frac{\mu_m}{KT_{in}}|\overrightarrow{v_m}|^2 \quad (17)$$

The dimensionless Bejan number quantifies the relative importance of heat transfer irreversibility in a system, it aids to analyzing and optimizing the efficiency of heat transfer processes, and is defined as [24]:

$$Be = \frac{S_{gen,T}}{S_{gen}} \quad (18)$$

The specific heat, density, thermal conductivity, thermal expansion coefficient, and viscosity of the copper-water nanofluid are determined using the following equations:

$$\rho_{nf} = (1-\varphi)\rho_f + \varphi\rho_{np} \quad (19)$$

$$\rho_{nf}Cp_{nf} = (1-\varphi_{np})\rho_f Cp_f + \varphi_{np}\rho_{np}Cp_{np} \quad (20)$$

$$\frac{k_{nf}}{k_f} = \left[\frac{(k_{np}+2k_f)+2\varphi(k_f-k_{np})}{(k_{np}+2k_f)+\varphi(k_f-k_{np})}\right] \quad (21)$$

$$\rho_{nf}\beta_{nf} = (1-\varphi_{np})\rho_f\beta_f + \varphi_{np}\rho_{np}\beta_{np} \quad (22)$$

$$\mu_{nf} = \mu_f(1-\varphi)^{-2.5} \quad (23)$$

The dimensionless form of variables used is given below:

$$X = \frac{x}{L},\ Y = \frac{y}{L},\ Z = \frac{z}{L},\ V = \frac{u}{u_0},\ \Theta = \frac{T-T_c}{T_h-T_c}$$

The boundary conditions are taken to be:

- The bottom wall of the fin:
  $T=T_h$
- The inlet (velocity inlet):
  $u=U_0$; $v=w=0$; $T=T_0$
- The outlet (outflow):
  $\frac{\partial u}{\partial x} = \frac{\partial v}{\partial y} = \frac{\partial w}{\partial z} = 0$; $\frac{\partial T}{\partial x} = 0$
- The rest of the walls (adiabatic):
  $u = v = w = 0$; $\frac{\partial T}{\partial x} = \frac{\partial T}{\partial y} = \frac{\partial T}{\partial z} = 0$

4. NUMERICAL FORMULATION

The Ansys-fluent version 14.5 software was utilized in order to carry out the numerical simulation, which uses the finite volume method as a discretization process equation that govern the flow. It was decided to go with the second-order upwind method combined with the Simple algorithm. The Boussinesq approximation model is used to describe the variation in density of the flow within the system, while the Darcy-Forchheimer model is used to describe the porous zone. In each of the cases, convergence of the solution was checked, and the convergence residuals were found to be less than 10^{-6}. This stringent criterion not only ensure numerical stability but also attests to the accurate representation of physical phenomena, emphasizing the precision of the results.

To analyze and assess proper grid independence of the numerical solution, five different grids consisting of 40×40×40, 50×50×50, 60×60×60, 70×70×70 and 80×80×80 grids in the x, y, and z directions, respectively, are tested with acceptable resolution near the walls of the cavity and the fin to capture the flow behavior (Figure 2) accurately. This refinement is required in this region, where viscous effects are dominant and crucial for capturing accurate velocity and pressure gradients. The results obtained given in (Table 2) and (Figure 3) show that the difference between the Nu_{avg} and the velocity variation of the last two grids is negligible. Hence, to achieve appropriate results with high precision and to save computing time, the grid size of 70×70×70 is chosen as the optimal grid.

Table 2. Results of grid independence test

Mesh	**40^3**	**50^3**	**60^3**	**70^3**	**80^3**
Nu_{avg}	22.80	23.45	23.53	23.60	23.61

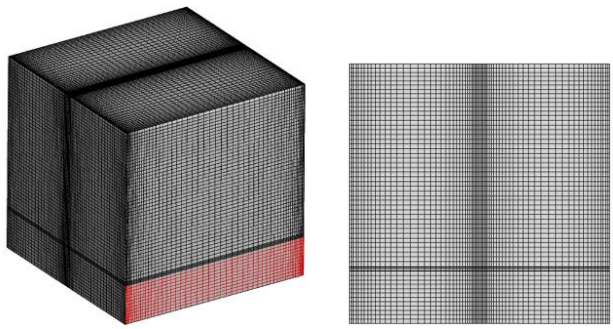

(3D) (2D)

Figure 2. The meshed geometry

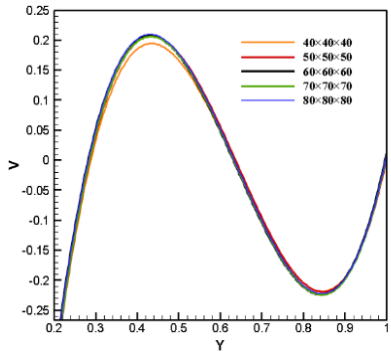

Figure 3. Grid independence study

The validation of the Fluent calculation code began with a comparison of the results obtained by our team with the findings that had previously been published by Kashyap and Dass [25] and Darzi et al. [26] considering the two-phase mixed convection using nanofluid in a cavity. This comparison

can be seen in Figure 4(a). Figure 4 shows the results of an additional validation that was performed for natural convection and buoyancy-induced flow using the nanofluid (Jahanshahi et al. [12] and Al-Rashed et al. [27]). (b). It has been noticed that the current findings are in remarkable agreement with the investigations that were covered in a previous discussion. Additionally, streamlines are depicted in Figure 5 of the figure. Clearly demonstrate a high level of concordance with the numerical data provided by Selimefendigil and Öztop [28].

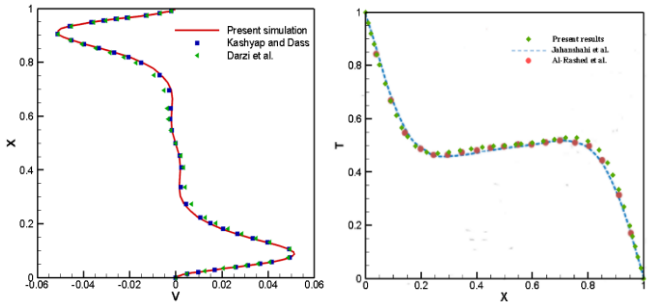

(a) (b)

Figure 4. Comparison between the present result and the result of (a) [21-22] and (b) [12-23]

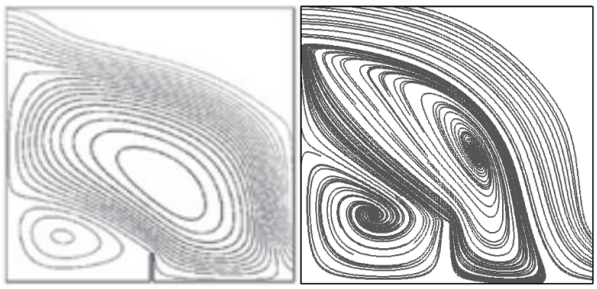

(a) (b)

Figure 5. Comparison of the streamlines for a cavity with a fin, (a) Selimefendigil and Öztop [28], (b) present study

5. RESULT AND DISCUSSION

The research involved examining various parameters, including the range of 10^{-4} to 10^{-1} for Da, 0.2 to 0.4 for ε, and 0 to 0.08 for φ. This section provides a comprehensive discussion of how these parameters influence heat transfer.

5.1 Darcy number effect

The calculation for different values of the Darcy number will be done to examine its influence on the mixed convection flow (Da=10^{-1}, 10^{-2}, 10^{-3}, and 10^{-4}), where Reynolds number (Re) and porosity (ε) are kept constant (Re=600 and ε=0.4), as well as the geometrical parameters of the cavity.

In porous media, the Da number represents the relative effect of the permeability as the fluid passes through it, where high Da values denote a higher permeability and vice versa. It also indicates how dominant the inertial forces are compared to the viscous forces in determining the fluid flow behavior [29]. The effects of Da on the average Nu_{avg}, Be, and S_{gen}, respectively, can be seen in Figure 6. It is observed that when Da is increased, the Nu_{avg} also increases for any value of φ, and the impact of Da on the Nu_{avg} is evident when the value of Da is raised from 10^{-4} to 10^{-3}. However, the increase in Nu_{avg} becomes almost negligible for higher values of Da. Higher Da makes the flow more dominated by inertial forces than viscous forces, which offers the nanofluid a better chance to flow faster in the porous region. Due to these higher inertial forces, the fluid can enter deeper into the porous structure and be interconnected with a larger heated surface area, promoting better mixing and more effectively carrying the heat away from the heated wall. This necessarily leads to improving convection flow and overall heat transfer, indicating higher Nu_{avg}. Also, at a constant value of Da, the Nu_{avg} increases when the φ increases, proving that adding nanoparticles signifies a higher thermal conductivity and improves heat transfer. It implies that the Nu_{avg} varies steadily and linearly with the φ for all cases of Da.

Figure 6(b) illustrates the variation of S_{gen} as a function of φ for different Da. We notice that by decreasing the Da, S_{gen} decreases due to increased flow resistance and decreased speed (velocity gradients). Besides, for all values of Da, φ effectively reduces S_{gen}.

Figure 6(c) depicts the variation of Be against φ for different values of Da. It is observed that the Be values at Da=10^{-1} and 10^{-2} are almost the same, while a noticeable difference is found at Da=10^{-3} and 10^{-4}. However, all these values are higher than 0.7, which means that the total entropy generation in the system is dominated by heat transfer irreversibility. This explains why the Be increases as the Da increases. In addition, for a given value of Da, the enhancement of φ causes the Be to increase slightly.

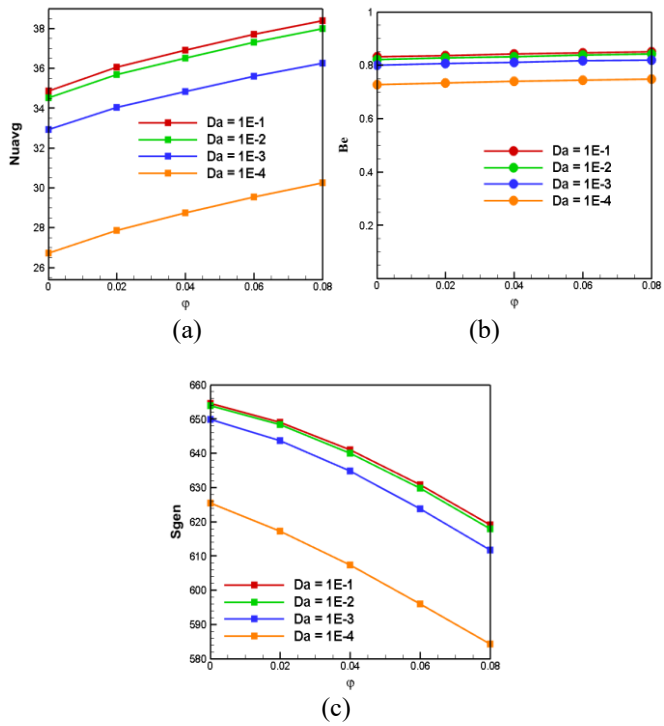

(a) (b)

(c)

Figure 6. Variation of Nu_{avg} (a), Be (b), and total entropy generation (c) versus φ for different Da at Re=600 and ε=0.4

The effects of Da on the streamlines and isotherms within the cavity for φ=4%, Re=600, and ε=0.4, are presented in Figure 7. As shown in the streamlines, three vortices of different sizes are created, the largest in the center and the others at the corners of the cavity. As the Da increases, the strength of the vortices increases, which means a better convection flow regime is created. Furthermore, the Da has a

clear impact on the isotherms, so that the more Da increases, the cavity's temperature distribution is improved, and the isothermal lines generated from the heated surface extend more and more over the cavity allowing the fluid to carry the heat easily at lower temperatures.

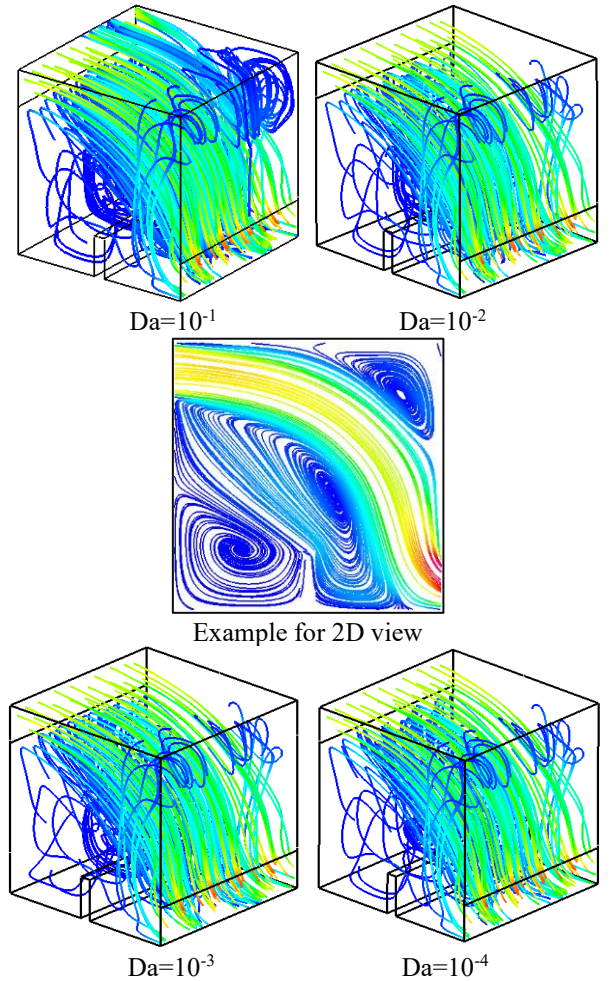

Figure 7. Isotherms (a) and streamlines (b) for different values of Da at Re=600, φ=4% and ε=0.4

Figure 8 illustrates the distribution of the Nu_{local} along the fin for different Da at Re=600, φ=4%, and ε=0.4. According to this figure, the local Nusselt number increased strongly when heading from bottom to the top of the fin due to the increase in surface area exposed to the fluid, which increases the heat transfer rate between the solid surface and the surrounding fluid, promoting a better convection.

The variation of the Nu_{local} versus distance along the heated surface for Re=600, ε=0.4, and φ=4% and for different Da is shown in Figure 9. It is observed that the heat transfer rate reached its maximum at the middle of the cavity due to the enhancement of convection flow, and the rate is minimum near the adiabatic walls due to boundary layer effects for all values of Da. It is also observed that Nu_{local} increases for high Da, which confirm what we explained before.

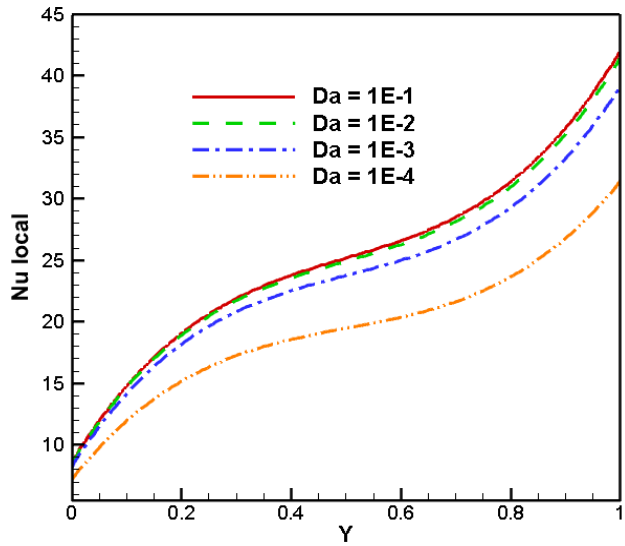

Figure 8. Distribution of the local Nusselt number along the fin for different Da at Re=600, φ=4% and ε=0.4

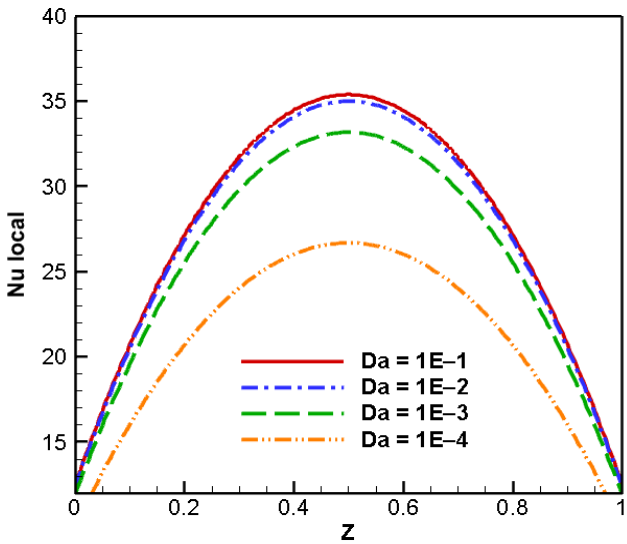

Figure 9. Distribution of the local Nusselt number along the heated surface from back to the front side for different Da at Re=600, φ=4%, and ε=0.4

5.2 The porosity effects

The effects of modifying the porosity of the medium on the Nu_{avg}, S_{gen}, and Be are shown in Figure 10. Different porosity

values (ε=0.2, 0.4, 0.6, and 0.8) are investigated for different φ. It can be observed that the Nu_{avg} increases when a larger porosity ratio is used. Since porosity measures the empty space within the medium, the amount of void spaces increases as the porosity ratio increases. This implies more space for the fluid to flow through, which might increase convection and heat transfer.

Figure 10(b) reveals the variation of S_{gen} with φ for different ε. As illustrated, S_{gen} increases by decreasing the porosity due to the rise in temperature gradients since the convection is weak, which leads to higher rates of entropy generation.

Figure 10(c) reveals the effects of the Be on the φ for different Da. High values of ε indicate a predominance of convective heat transfer, which means higher fluid perturbation emerges. As fluid flows through the pores of the material, it forms a thermal boundary layer along the solid-fluid interface. This boundary layer is where most of the convective heat transfer take place. With higher ε, the thickness of this boundary layer may decrease due to increased fluid flow and turbulence, leading to enhance heat transfer. This results an increase in temperature gradients. Therefore, the cavity's larger heat transfer irreversibility makes the Be rise. In addition, there is a slight augmentation of Be when increasing φ.

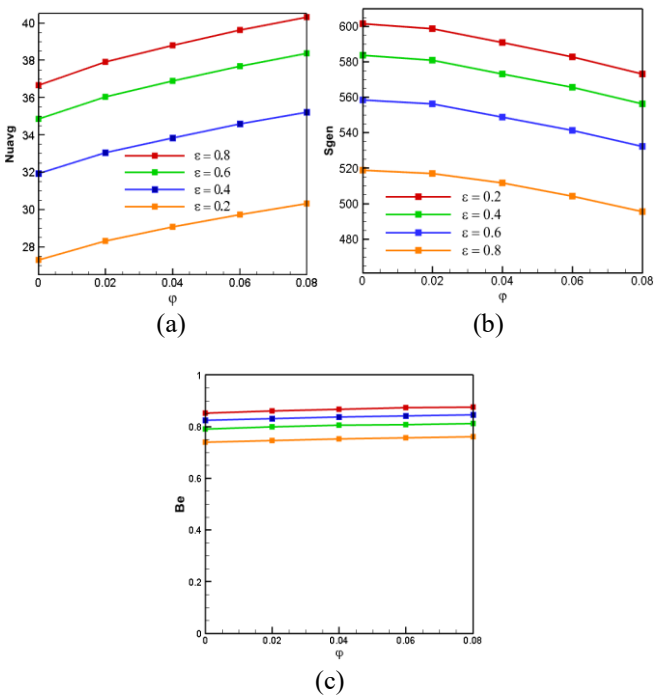

Figure 10. Variation of Nu_{avg} (a), Be (b), and total entropy generation (c) versus φ for different values of ε at Re=600 and $Da=10^{-1}$

Figure 11 displays the impact of the ε on fluid flow and heat transfer in terms of isotherms and streamlines. it can be seen that the ε has a significant effect on isotherms since convection is considerable at high ε values and it is accompanied by decreasing viscous effects; the intensity of the temperature gradients along the fin as it is the main source of heat diffusion become less by increasing the ε values.

On the other hand, streamlines show three recirculation cells with a major vortex at the middle of the cavity, and two other vortices at the corners are generated. The size of the vortex near the porous medium increased by increasing the ε, and the fluid circulation in this area became significant.

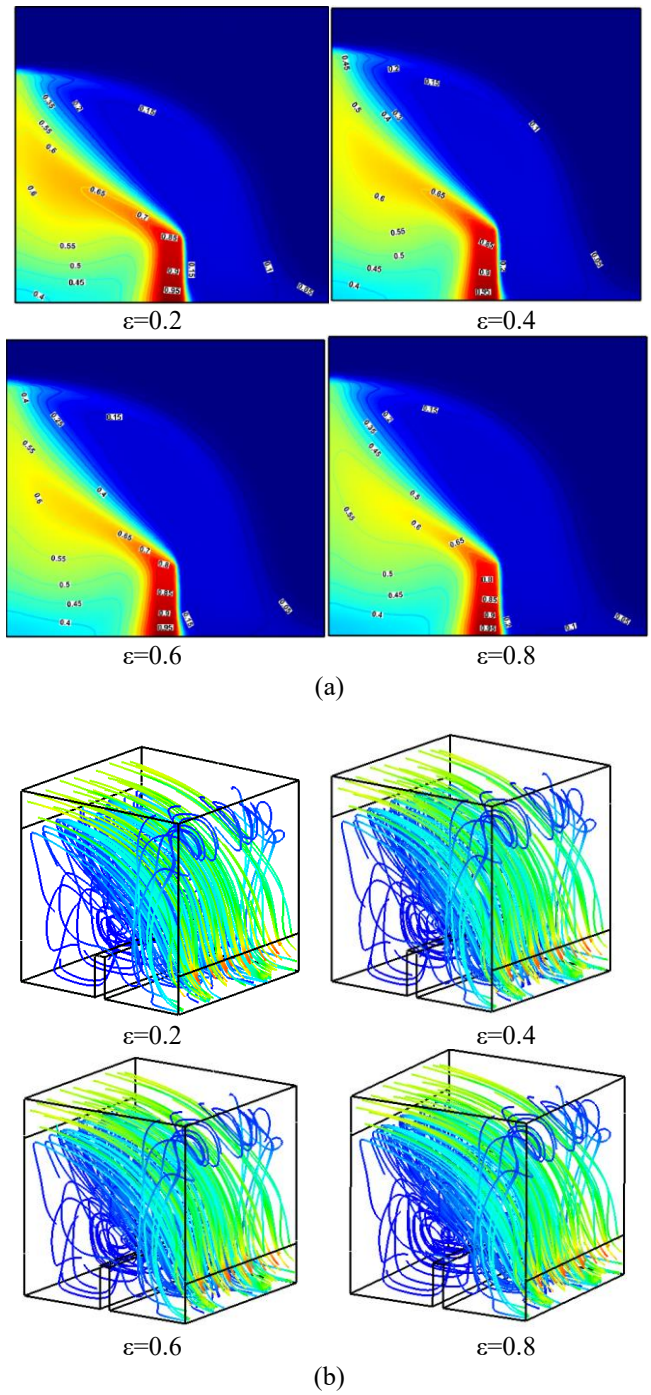

Figure 11. Isotherms (a) and streamlines (b) for different values of ε at Re=600, φ=4% and $Da=10^{-1}$

5.3 Correlation

Finally, two correlations for Nu are done in terms of the pertinent parameters, Re, Da, φ and the porosity are presented in Figure 12. The correlations are expressed as follows:

$$Nu = 0.328 Re^{0.671} Da^{0.0380} (1+\varphi)^{1.291} \quad (24)$$

$$Nu = 0.286\, Re^{0.774}\, \varepsilon^{0.027}\, (1+\varphi)^{1.235} \quad (25)$$

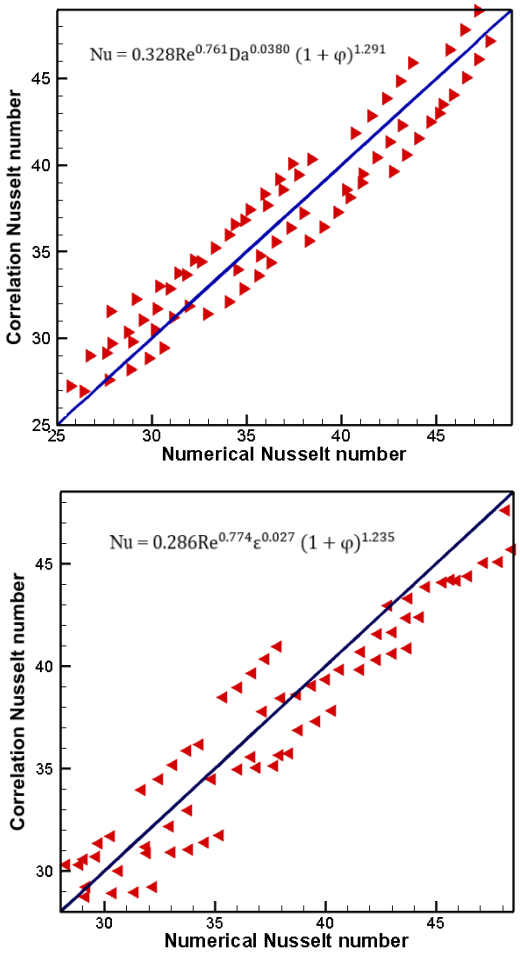

Figure 12. Comparison between the numerical results and correlation

6. CONCLUSION

The simulation of mixed convection within an open square cavity filled with Cu-water nanofluid and featuring an internally finned structure enveloped in a porous medium was considered.

Important parameters, including Re, Da, φ, and ε, were examined, yielding the following conclusions:

- Increasing the nanofluid's solid volume fraction enhanced convective heat transfer but negatively impacted total entropy generation.
- Higher Da led to an increase in Nu_{avg}, total entropy generation, and Be numbers.
- Manipulating ε increased the Nu_{avg} and the Be numbers but reduced the total entropy generation.
- Higher solid volumes fraction in the nanofluid improved heat transfer.
- The presence of the internal fin and the porous media notably enhance the heat exchange.
- Incorporating nanofluids into heat and cooling systems could lead to significant improvements in heat transfer efficiency, ultimately contributing to sustainability goals.
- The observed impact of material porosity on heat transfer highlights the importance of material selection and design.

The study likely made simplifications and assumptions to model the complex system, such as assuming steady-state conditions or neglecting certain effects like thermal radiation. These simplifications might not fully capture the real-world behavior of the system. The range of parameters investigated (Darcy numbers, porosity, solid volume fraction) may not cover the full spectrum of potential values encountered in real-world systems.

Investigating the effects of varying cavity geometries, fin configurations, and porous medium structures on heat transfer and entropy generation would help in understanding the system's behavior under different conditions.

REFERENCES

[1] Choi, S.U.S. (1995). Enhancing thermal conductivity of fluids with nanoparticles. American Society of Mechanical Engineers, Fluids Engineering Division, 231: 99-105.

[2] Saidur, R., Leong, K.Y., Mohammed, H.A. (2011). A review on applications and challenges of nanofluids. Renewable and Sustainable Energy Reviews, 15(3): 1646-1668. https://doi.org/10.1016/j.rser.2010.11.035

[3] Ruvo, T.H., Saha, S., Mojumder, S., Saha, S. (2023). Mixed convection in an open T-shaped cavity utilizing the effect of different inflow conditions with Al_2O_3-water nanofluid flow. Results in Engineering, 17: 100862. https://doi.org/10.1016/j.rineng.2022.100862

[4] Nayak, R.K., Bhattacharyya, S., Pop, I. (2016). Heat transfer and entropy generation in mixed convection of a nanofluid within an inclined skewed cavity. International Journal of Heat and Mass Transfer, 102: 596-609. https://doi.org/10.1016/j.ijheatmasstransfer.2016.06.049

[5] Tian, Z., Shahsavar, A., Al-Rashed, A.A.A.A., Rostami, S. (2021). Numerical simulation of nanofluid convective heat transfer in an oblique cavity with conductive edges equipped with a constant temperature heat source: Entropy production analysis. Computers & Mathematics with Applications, 81: 725-736. https://doi.org/10.1016/j.camwa.2019.12.007

[6] Izadi, M., Behzadmehr, A., Shahmardan, M.M. (2015).Effects of inclination angle on mixed convection heat transfer of a nanofluid in a square cavity. International Journal for Computational Methods in Engineering Science and Mechanics, 16(1): 11-21. https://doi.org/10.1080/15502287.2014.976674

[7] Selimefendigil, F., Öztop, H.F. (2018). Mixed convection of nanofluids in a three dimensional cavity with two adiabatic inner rotating cylinders. International Journal of Heat and Mass Transfer, 117: 331-343. https://doi.org/10.1016/j.ijheatmasstransfer.2017.09.116

[8] Shulepova, E.V. , Sheremet, M.A., Oztop, H.F., Abu-Hamdeh, N. (2020). Mixed convection of Al_2O_3–H_2O nanoliquid in a square chamber with complicated fin. International Journal of Mechanical Sciences, 165: 105192. https://doi.org/10.1016/j.ijmecsci.2019.105192

[9] Cho, C.C. (2018). Heat transfer and entropy generation of mixed convection flow in Cu-water nanofluid-filled lid-driven cavity with wavy surface. International Journal of Heat and Mass Transfer, 119: 163-174. https://doi.org/10.1016/j.ijheatmasstransfer.2017.11.090

[10] Hussain, S., Ahmed, S.E., Akbar, T. (2017). Entropy generation analysis in MHD mixed convection of hybrid nanofluid in an open cavity with a horizontal channel

containing an adiabatic obstacle. International Journal of Heat and Mass Transfer, 114: 1054-1066. https://doi.org/10.1016/j.ijheatmasstransfer.2017.06.135

[11] Benkhedda, M., Boufendi, T., Touahri, S. (2018). Laminar mixed convective heat transfer enhancement by using Ag-TiO_2-water hybrid Nanofluid in a heated horizontal annulus. Heat Mass Transfer, 54: 2799-2814. https://doi.org/10.1007/s00231-018-2302-x

[12] Jahanshahi, M., Hosseinizadeh, S.F., Alipanah, M., Dehghani, A., Vakilinejad, G.R. (2010). Numerical simulation of free convection based on experimental measured conductivity in a square cavity using water/SiO_2 nanofluid. International Communications in Heat and Mass Transfer, 37(6): 687-694. https://doi.org/10.1016/j.icheatmasstransfer.2010.03.010

[13] Chamkha, A.J., Abu-Nada, E. (2012). Mixed convection flow in single- and double-lid driven square cavities filled with water-Al_2O_3 nanofluid: Effect of viscosity models. European Journal of Mechanics - B/Fluids, 36: 82-96. https://doi.org/10.1016/j.euromechflu.2012.03.005

[14] Çolak, E., Ekici, Ö., Öztop, H.F. (2021). Mixed convection in a lid-driven cavity with partially heated porous block. International Communications in Heat and Mass Transfer, 126: 105450. https://doi.org/10.1016/j.icheatmasstransfer.2021.105450

[15] Sheremet, M.A., Roşca, N.C., Roşca, A.V., Pop, I. (2018). Mixed convection heat transfer in a square porous cavity filled with a nanofluid with suction/injection effect. Computers & Mathematics with Applications, 76(11-12): 2665-2677. https://doi.org/10.1016/j.camwa.2018.08.069

[16] Tham, L., Nazar, R., Pop, I. (2016). Mixed convection flow over a horizontal circular cylinder with constant heat flux embedded in a porous medium filled by a nanofluid : Buongiorno – Darcy model. Heat Mass Transfer, 52: 1983-1991. https://doi.org/10.1007/s00231-015-1720-2

[17] Siavashi, M., Yousofvand, R., Rezanejad, S. (2018). Nanofluid and porous fins effect on natural convection and entropy generation of flow inside a cavity. Advanced Powder Technology, 29(1): 142-156. https://doi.org/10.1016/j.apt.2017.10.021

[18] Rajarathinam M., Nithyadevi, N. (2017). Heat transfer enhancement of Cu-water nanofluid in an inclined porous cavity with internal heat generation. Thermal Science and Engineering Progress, 4: 35-44. https://doi.org/10.1016/j.tsep.2017.08.003

[19] Emami, R.Y., Siavashi, M., Moghaddam, G.S. (2018). The effect of inclination angle and hot wall configuration on Cu-water nanofluid natural convection inside a porous square cavity. Advanced Powder Technology, 29(3): 519-536. https://doi.org/10.1016/j.apt.2017.10.027

[20] Mahian, O., Kolsi, L., Amani, M., Estellé, P., Ahmadi, G., Kleinstreuer, C., Marshall, J.S., Siavashi, M., Taylor, R.A., Niazmand, H., Wongwises, S., Hayat, T., Kolanjiyil, A., Kasaeian, A., Pop, I. (2019). Recent advances in modeling and simulation of nanofluid flows-Part I: Fundamentals and theory. Physics Reports, 790: 1-48. https://doi.org/10.1016/j.physrep.2018.11.004

[21] Hoseininejad, F., Dinarvand, S., Yazdi, M.E. (2021). Manninen's mixture model for conjugate conduction and mixed convection heat transfer of a nanofluid in a rotational/stationary circular enclosure. International Journal of Numerical Methods for Heat & Fluid Flow, 31(5): 1662-1694. https://doi.org/10.1108/HFF-05-2020-0301

[22] Stephens, S.D.G. (1985). Book reviews. International Journal of Language Communication Disorders, 20(1): 91-111. https://doi.org/10.3109/13682828509012252

[23] Roy, M., Roy, S., Basak, T. (2015). Analysis of entropy generation on mixed convection in square enclosures for various horizontal or vertical moving wall(s). International Communications in Heat and Mass Transfer, 68: 258-266. https://doi.org/10.1016/j.icheatmasstransfer.2015.08.023

[24] Cho, C.C. (2014). Heat transfer and entropy generation of natural convection in nanofluid-filled square cavity with partially-heated wavy surface. International Journal of Heat and Mass Transfer, 77: 818-827. https://doi.org/10.1016/j.ijheatmasstransfer.2014.05.063

[25] Kashyap D., Dass, A.K. (2019). Effect of boundary conditions on heat transfer and entropy generation during two-phase mixed convection hybrid Al_2O_3-Cu/water nanofluid flow in a cavity. International Journal of Mechanical Sciences, 157-158: 45-59. https://doi.org/10.1016/j.ijmecsci.2019.04.014

[26] Darzi, A.A.R., Farhadi, M., Lavasani, A.M. (2016). Two phase mixture model of nano-enhanced mixed convection heat transfer in finned enclosure. Chemical Engineering Research and Design, 111: 294-304. https://doi.org/10.1016/j.cherd.2016.05.019

[27] Al-Rashed, A.A.A.A., Kalidasan, K., Kolsi, L., Velkennedy, R., Aydi, A., Hussein, A.K., Malekshah, E.H. (2018). Mixed convection and entropy generation in a nanofluid filled cubical open cavity with a central isothermal block. International Journal of Mechanical Sciences, 135: 362-375. https://doi.org/10.1016/j.ijmecsci.2017.11.033

[28] Selimefendigil, F., Öztop, H.F. (2012). Fuzzy-based estimation of mixed convection heat transfer in a square cavity in the presence of an adiabatic inclined fin. International Communications in Heat and Mass Transfer, 39(10): 1639-1646. https://doi.org/10.1016/j.icheatmasstransfer.2012.10.006

[29] Nithiarasu, P., Seetharamu, K.N., Sundararajan, T. (1997). Natural convective heat transfer in a fluid saturated variable porosity medium. International Journal of Heat and Mass Transfer, 40(16): 3955-3967. https://doi.org/10.1016/S0017-9310(97)00008-2

NOMENCLATURE

Be	Bejan number
Cd	inertia coefficient
Cp	specific heat, J. kg^{-1}. K^{-1}
Da	darcy number
g	gravitational acceleration, $m.s^{-2}$
k	thermal conductivity, $W.m^{-1}$. K^{-1}
L	cavity length, m
Nu	Nusselt number
Re	Reynolds number
T	temperature, K

u,v,w	velocity components, $m.s^{-1}$
V	dimensionless velocity
x,y,z	Cartesian coordinates, m
X,Y,Z	dimensionless Cartesian coordinates, m
U_0	inlet velocity, $m.s^{-1}$

Greek symbols

β	thermal expansion coefficient, K^{-1}
ε	porosity
φ	solid volume fraction
Θ	dimensionless temperature
ρ	density, $kg.m^{-3}$
μ	dynamic viscosity, $kg.\ m^{-1}.\ s^{-1}$
Δ	difference
Γ	thermal diffusivity coefficient

Subscripts

avg	average
c	cold
dr	drift of water
f	fluid (pure water)
m	mixture
np	nanoparticle
p	particle